Low-energy optical excitation in rare-earth hexaborides

Shin-ichi Kimura
Ultraviolet Synchrotron Orbital Radiation Facility, Institute for Molecular Science, Myodaiji, Okazaki 444, Japan

Takao Nanba
Department of Physics, Faculty of Science, Kobe University, 1-1 Rokkodai, Nada-ku, Kobe 657, Japan

Satoru Kunii and Tadao Kasuya
Department of Physics, Faculty of Science, Tohoku University, Aramaki Aza Aoba, Aoba-ku, Sendai 980, Japan
(Received 7 December 1993)

Reflectivity spectra of trivalent rare-earth hexaborides (RB_6; R=La, Ce, Pr, Nd, Gd, Tb, Dy, Ho, and Y) and mixed-valent SmB_6 have been measured in the photon energy region from 1 meV to 40 eV at 300 and 9 K. We discuss the absorption structure due to conduction electrons. Even in LaB_6 and YB_6, which have no $4f$ electrons, the optical conductivity spectra were not fitted by a simple Drude model and a frequency-dependent relaxation time was observed. This was attributed to the electron-phonon and electron-electron scattering. In RB_6 with $4f$ electrons, a common absorption structure was observed at the energy position of about 0.6 eV. The intensity was found to be almost proportional to the $4f$ spin angular momentum. From the f-sum rule, the absorption was found to be due to the conduction electrons. The origin was assigned to be due to the transition or to the relevant exciton absorption from the saddle points of Σ_1 at the neck point to the saddle points of Γ_{12} and Γ_{25} assisted by the scattering of the intra-atomic $5d$-$4f$ Coulomb exchange interaction, in particular enhanced in the heavy RB_6 compounds by the lattice instability. In SmB_6, the absorption that was seen in trivalent RB_6's was also observed in addition to absorptions from $4f$ states of Sm^{2+} to $5d$ states and from $5d$ to $4f$ in Sm^{3+}. This is thought to mean that the Fermi level of SmB_6 is located at the same energy position in the band structure as that of the trivalent RB_6.

I. INTRODUCTION

Rare-earth hexaborides (RB_6) have a variety of interesting physical properties. For example, CeB_6 shows dense Kondo and heavy-fermion properties,[1] SmB_6 is a typical valence-fluctuating compound,[2] and EuB_6 has ferromagnetic semiconducting character.[3] Therefore many experiments for investigation of the origin of the properties have been done. The optical properties of these materials, however, have been scarcely investigated.

Investigation of the reflectivity spectra of RB_6 was done for LaB_6, PrB_6, SmB_6, and NdB_6 by Kierzek-Pecold in a narrow energy range from 1 to 5.6 eV.[4] In the investigation, the plasma edge of the conduction electrons was observed at 2 eV for all these materials. After that, the reflectivity spectra of LaB_6 and EuB_6 were measured in the wider energy range from 0.05 to 18 eV and the optical constants were derived from these reflectivity spectra by Gurin *et al.*[5] Travaglini and Wachter measured the reflectivity spectrum of SmB_6 in the energy range from 1 meV to 12 eV at 300 and 4 K for investigation of the energy-gap state.[6] Optical measurements on other RB_6's have not yet been done to our knowledge.

We have measured the reflectivity spectra of all RB_6 single crystals. The purpose is to obtain information on the electronic structure,[7,8] on the optical phonon of YbB_6,[9] and on the origin of the anomalous infrared absorption due to the conduction electrons in light RB_6's from LaB_6 to GdB_6.[10] In our previous paper, we reported the existence of infrared absorption of the compounds RB_6 from CeB_6 to GdB_6 which have less than half filling of the $4f$ electron orbital and concluded that it was due to the conduction electrons.[10]

Recently, Segawa *et al.* succeeded in making single crystals of TbB_6, DyB_6, and HoB_6.[11] So we measured the reflectivity spectra of these materials in the energy range from 1 meV to 40 eV. The spectra of all RB_6's in the energy range above 2 eV, which are due to the interband transitions, were discussed in our separate paper.[8] In this paper, we analyze and discuss the conduction-electron absorption of trivalent RB_6's (R =La, Ce, Pr, Nd, Gd, Tb, Dy, and Ho) and mixed-valent SmB_6. First we will discuss the frequency-dependent optical mass and relaxation time of LaB_6 and YB_6 which are generally thought to be normal metals with one carrier per rare-earth atom, in Sec. IV A. Second we will show the results and discuss the origin of the absorption structure at 0.6 eV which is seen in all RB_6's with occupied $4f$ electron orbitals in Sec. IV B. Last, the absorption structure below 2 eV in SmB_6 will be discussed in Sec. IV C.

The crystal structure of RB_6 is CaB_6 type with the space group P_m3_m (O_h), in which the B_6 molecule has the octahedron structure. The positions of R and B_6 octahedra correspond to those of Cs and Cl sites, respectively, in the CsCl structure. The B_6 network is made by strong covalent bonds; on the other hand, the bonding

between R and B_6 is metallic. The crystalline bonding is mainly made by the B_6 network.

From the study of the electronic structure of metal hexaborides (MB_6; M = metal) by Longuet-Higgins and de Roberts,[12] the valence number of the B_6 octahedron is -2. Therefore MB_6 with M^{2+} becomes an insulator or a semiconductor and MB_6 with M^{3+} a monovalent metal. Most of the RB_6 compounds belong to the M^{3+} group because of the R^{3+} ion. In this case, the conduction band consists of the bonding state between R $5d$ (e_g) and B_6 $2p$ (t_{2u}).

II. EXPERIMENTAL METHOD

RB_6 samples were grown as single crystals by the crucible-free vertical floating-zone method.[13] The obtained crystals were cut into disks of about 7 mm diameter and 1 mm thickness by an electric spark cutter and polished up to mirror surfaces with Carborundum and alumina powders for reflectivity measurements.

We measured the reflectivity spectra in the wide energy range between 1 meV in the far-infrared region and 40 eV in the vacuum-ultraviolet region. The measurements in the far-infrared region from 1 to 30 meV and in the vacuum-ultraviolet region from 4 to 40 eV were done at two synchrotron radiation (SR) facilities, UVSOR in the Institute for Molecular Science and SOR-RING in the Institute for Solid State Physics, the University of Tokyo, respectively. In the former, the SR light was monochromatized by a Martin-Puplett-type Fourier spectrometer and its intensity was detected by a Ge bolometer and an InSb hot-electron detector.[14] In the latter, the SR was monochromatized by a 1-m Seya-Namioka-type monochromator. In the intermediate energy region between 50 meV and 5 eV, appropriate combinations of conventional light sources, monochromators, and detectors were adopted. These combined experimental systems are listed in Table I.

The experimental error of the absolute value of the reflectivity was estimated at less than 1% in the energy region below 2 eV and less than 3% in the energy region above 2 eV. The energy resolution ($E/\Delta E$) was higher than 20 at each energy. The measurements were done at two different temperatures, 300 and 9 K, in the energy region below 5 eV. In this paper, we also discuss the difference between the spectra at 300 and 9 K.

Figure 1 shows the reflectivity spectra of trivalent RB_6's at both 300 and 9 K in the energy region from 50 meV to 40 eV. Below 50 meV, the reflectivity approaches 1 as the photon energy decreases. Note that the horizontal axis is in a logarithmic scale. In the figure, the plasma edge of trivalent RB_6 can be seen as a sharp dip structure in the spectrum at the common energy position of about 2 eV.

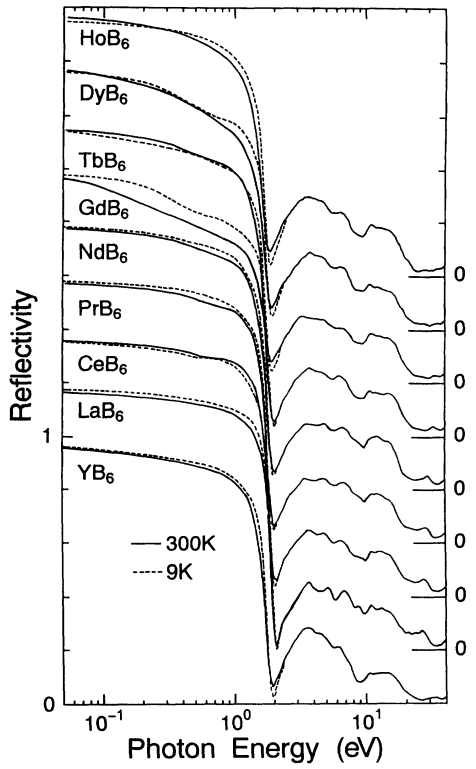

FIG. 1. Reflectivity spectra of trivalent rare-earth hexaborides (RB_6, R = Y, La, Ce, Pr, Nd, Gd, Tb, Dy, and Ho) in the photon energy region from 50 meV to 40 eV at 300 and 9 K. The horizontal axis is drawn in a logarithmic scale.

III. ANALYSIS METHOD

A. Kramers-Kronig analysis

In this paper, we consider the low-energy electronic states using the optical conductivity and the effective electron number spectra. The optical conductivity spectrum, $\sigma(\hbar\omega)=\epsilon_2\hbar\omega/2$, was obtained by using a Kramers-Kronig (KK) transformation of the reflectivity

TABLE I. The optical measurement systems used.

Energy range	1–8.6 meV	2.5–30 meV	0.05–0.5 eV	0.3–0.7 eV	0.5–2.3 eV	1.7–4 eV	3.5–5.5 eV	4–40 eV
Light source	UVSOR		Globar lamp		Tungsten lamp		Deuterium lamp	SOR-RING
Monochromator	SPECAC Martin-Puplett		Hitachi Plane grating		Carl-Leiss LiF double prism			KOHZU 1-m Seya-Namioka
Detector	InSb hot electron	Ge bolometer	Ge-Cu bolometer	PbS photocell at 77 K	PbS photocell at 300 K		Photomultiplier	

spectrum. Here ε_2 is the imaginary part of the dielectric constant. The effective electron number as a function of the photon energy $N_{\text{eff}}(\hbar\omega)$ was obtained from the integration of the optical conductivity spectrum as

$$N_{\text{eff}}(\hbar\omega)=\frac{4m_0}{h^2e^2N_0}\int_0^{\hbar\omega}\sigma(\hbar\omega')d\hbar\omega' . \quad (1)$$

Here, m_0 is the rest mass of the electron, h the Planck constant, e the charge of the electron, and N_0 the number of unit cells per unit volume. The KK transformation requires a reflectivity spectrum for the whole photon energy range from zero to infinity in principle. But we have spectra only for a limited energy region. Thus we adopted two kinds of extrapolation functions in the energy regions below 1 meV and above 40 eV. In the energy region below 1 meV, we adopted a function of Hagen-Rubens' formula,[15]

$$R(\hbar\omega)=1-[2/\pi\sigma(0)]^{1/2}\times(\hbar\omega)^{1/2} ,$$

because of the metallic reflectivity spectrum. Here, $\sigma(0)$ means the dc conductivity from transport measurements. In the energy region above 40 eV, we adopted the usual extrapolation function for electronic interband transitions as used by Cardona and co-workers,[16] $R(\hbar\omega)=B\times(\hbar\omega)^{-4}$. Here, we decided the value for B so that the extrapolation function connects with the actual reflectivity spectra at 40 eV.

B. Expanded Drude formula

In this paper, we use the Drude formula for analysis of the reflectivity spectra. The real part (ε_1) and imaginary part (ε_2) of the dielectric constant are

$$\varepsilon_1=\varepsilon_{\text{opt}}-\frac{\omega_p^2\tau^2}{\omega^2\tau^2+1} , \quad (2)$$

$$\varepsilon_2=\frac{\omega_p^2\tau}{\omega(\omega^2\tau^2+1)} . \quad (3)$$

Here, τ is the relaxation time of the conduction electrons. ε_{opt} means the optical dielectric constant and shows the intensity of the interband transitions in the energy range above the plasma edge, for which the energy is about 2 eV in this case. ω_p means the plasma frequency, $\omega_p^2=4\pi e^2N/m_D$. Here, N is the number of conduction electrons per formula unit and m_D is the effective mass of conduction electrons estimated by the Drude model. The observed plasma frequency seen in the reflectivity spectrum, the so-called effective plasma frequency ω_p^*, is given by $\omega_p^*=\omega_p/\sqrt{\varepsilon_{\text{opt}}}$. In other words, the interband transition screens the plasma frequency by ε_{opt}. ε_{opt} is derived from the next relation. In general the sum rule which is used to get the effective electron number N_{eff} is given by Eq. (1). This formula is the sum rule for the dispersion of the transverse wave, while the sum rule for the absorption of the longitudinal wave is obtained using the loss function $[-\text{Im}(1/\varepsilon);\varepsilon=\varepsilon_1+i\varepsilon_2]$ as

$$N_{\text{loss}}(\hbar\omega)=\frac{4m_0}{h^2e^2N_0}\int_0^{\hbar\omega}\hbar\omega'\left[-\text{Im}\left[\frac{1}{\varepsilon(\hbar\omega')}\right]\right]d\hbar\omega' . \quad (4)$$

The relation between these two kinds of sum rule is given by using ε_{opt} as

$$N_{\text{eff}}(\hbar\omega)=\varepsilon_{\text{opt}}^2\times N_{\text{loss}}(\hbar\omega) . \quad (5)$$

Next, we show how to derive the frequency dependence of the relaxation time and the optical mass from the dielectric constants. In general, the actual spectrum cannot be fitted by the simple Drude model in which both τ and ω_p are constant. However, if the conduction band is not complex, it is a good approximation and each of the relaxation time and the optical mass has a weak frequency dependence. The modified Drude model in which both τ and ω_p depend on ω satisfies the KK relation when they are determined to fit the experimental ε_1 and ε_2 values. In monovalent metals such as LaB_6, the conduction band consists of bands of a single character. So it is thought that the conduction-electron absorption can be interpreted by a single Drude model. Therefore it is thought that the investigation of the frequency dependence of the optical mass and the relaxation time is very useful. In LaB_6, however, three identical occupied bands with the bottoms at three X points are connected to each other by small necks. However, unoccupied bands are composed with more complexity of many different characters with many singular points. These effects are considered later in more detail.

From Eqs. (2) and (3), τ and m_D/m are obtained as

$$\tau=\frac{\varepsilon_{\text{opt}}-\varepsilon_1}{\omega\varepsilon_2} , \quad (6)$$

$$\frac{m_D}{m_0}=\frac{4\pi Ne^2}{m_0}\left[\frac{\omega^2\varepsilon_2^2}{\varepsilon_{\text{opt}}-\varepsilon_1}+\omega^2(\varepsilon_{\text{opt}}-\varepsilon_1)\right]^{-1} , \quad (7)$$

in which N may be assumed to be frequency independent. By using these functions, the frequency-dependent optical mass and relaxation time are derived from the reflectivity spectra.

IV. RESULTS AND DISCUSSION

A. Drude absorption of LaB_6 and YB_6

First, we show the results for and discuss the conduction-electron absorption of LaB_6 and YB_6. The optical conductivity spectra of both materials at 300 and 9 K are shown in Fig. 2. We may see that both of these materials' spectra are able to be roughly fitted by the simple Drude model, but it is impossible to fit exactly. This means that both spectra should be analyzed by the model with the frequency-dependent optical mass (m_D) and relaxation time (τ) given by Eqs. (7) and (6). The results are shown in Figs. 3(a) and 3(b). Here, the optical dielectric constant (ε_{opt}) was derived from Eqs. (1), (4), and (5). In LaB_6, ε_{opt} was 6.0 and in YB_6 $\varepsilon_{\text{opt}}=5.8$. The difference is thought to depend on whether an unoccu-

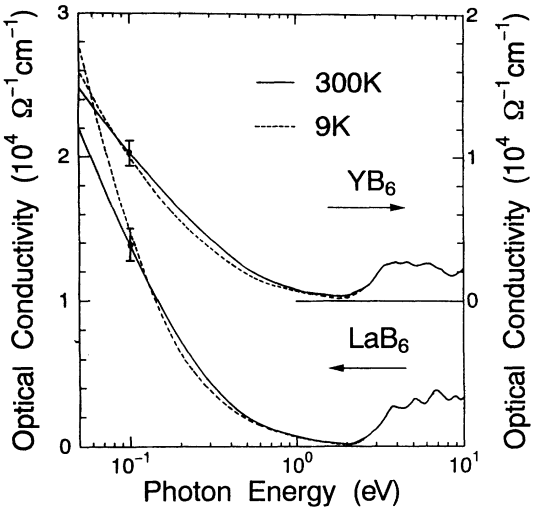

FIG. 2. Optical conductivity spectra of LaB_6 and YB_6 in the photon energy region from 50 meV to 10 eV at 300 and 9 K.

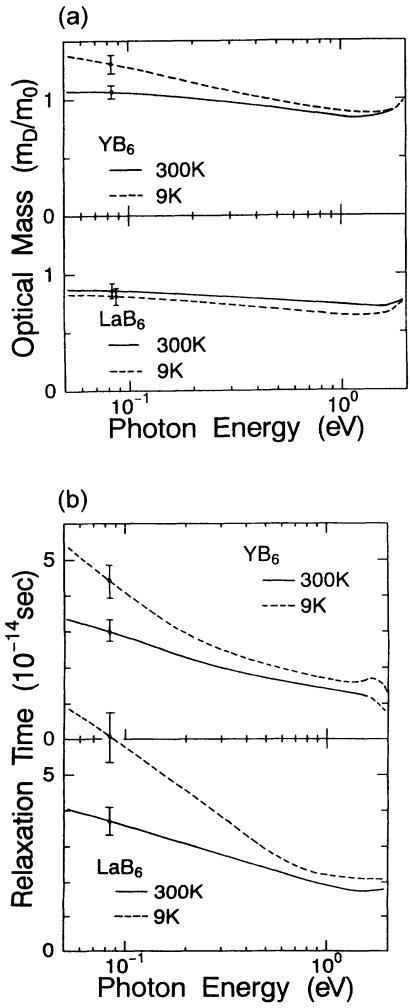

FIG. 3. Optical mass (a) and relaxation time (b) of LaB_6 and YB_6 as a function of the photon energy.

pied $4f$ state exists or not. In LaB_6, which has an unoccupied $4f$ state, the transition from the B $2s,2p$ bonding state to $4f$ is seen in the energy region around 10 eV as shown in Ref. 8. In these figures, m_D of LaB_6 and YB_6 have little frequency dependence, but τ has a strong dependence. The reason is discussed below.

The study of the absorption due to conduction electrons has been done on noble metals and alkali metals. It is known that even in these typical metals it is not possible to fit the data completely by a single simple Drude model. The reason is thought to lie in the frequency dependence of the electron-phonon scattering,[17] the electron-electron scattering,[18] and the surface plasmon,[19] etc. In the present case, the surface plasmon is hardly thought to be the origin because of the near-normal-incidence reflectivity measurement. For the case of electron-electron scattering, τ may be expressed as follows by using the Fermi liquid theory:[20]

$$\tau^{-1}=\tau_0^{-1}+\beta\omega^2 \ . \tag{8}$$

Here, τ_0 is the relaxation time at zero frequency, and therefore corresponds to the static conductivity, and β is a constant of the material.

In Ag and Cu, for example, τ in the energy range above 0.5 eV^2 was fitted by this function.[18] Recently Julien *et al.* showed that the reflectivity of a layered crystal, TiS_2, was satisfactorily fitted with Eq. (8).[21] Figure 4 shows τ as a function of the square of the energy in LaB_6 and YB_6. The relation $\tau^{-1}\propto\omega^2$ actually holds in the energy range from 0.5 to 1.1 eV. This means that the frequency dependence of τ in the high frequency region is mainly due to electron-electron scattering. This is consistent with the observed weak temperature dependence of the $\beta\omega^2$ term.

On the other hand, as seen in Fig. 3(b) the temperature dependence of τ between 0.05 and 0.5 eV is rather well fitted by the function $\tau_1\ln[\omega_0/(\omega+\omega_1)]$, where ω_1 is sufficiently smaller than 0.05 eV, and thus seems to correspond to the phonon frequency of La or Y. In these ma-

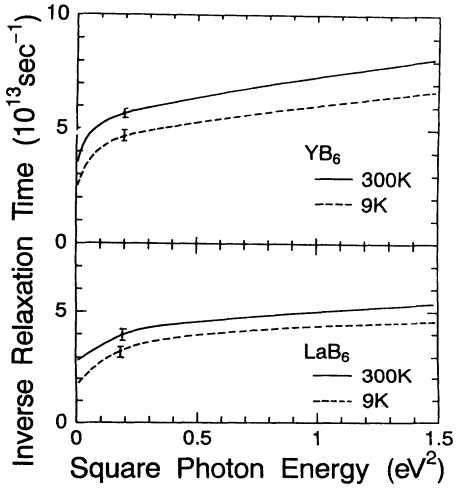

FIG. 4. Inverse relaxation time as a function of the squared photon energy of LaB_6 and YB_6.

terials, the lowest optical phonon mode is about 0.02 eV and the highest phonon mode for the B_6 molecule is near 0.15 eV.[22] The fitting parameters were $\tau_1=0.8\times10^{-14}$ sec and $\hbar\omega_0=12$ eV at 300 K and $\tau_1=1.95\times10^{-14}$ sec and $\hbar\omega_0=2.5$ eV at 9 K in LaB_6, $\tau_1=1.0\times10^{-14}$ sec and $\hbar\omega_0=2.5$ eV at 300 K and $\tau_1=2.1\times10^{-14}$ sec and $\hbar\omega_0=1.0$ eV at 9 K in YB_6. This part of the spectrum is thought to be due to the electron-phonon scattering. The observed temperature dependence also supports this picture. This weak ω dependence indicates that the intra-B_6-molecular vibrations scatter the conduction electrons weakly and this is also consistent with the weak temperature dependence of the static resistivity above 200 K.[23]

B. Infrared absorption of trivalent RB_6

In our previous paper, we reported that in the lighter RB_6's there is an anomalous absorption around 0.6 eV in which the intensity is proportional to the occupation number of $4f$ electrons.[10] This absorption structure was explained as due to the conduction electrons by consideration of the f-sum rule. But a detailed interpretation was not made. We measured the reflectivity spectra of the heavier RB_6's and found a similar absorption structure to the lighter RB_6's. In this section, we will discuss the origin of the absorption structure. All of the optical conductivity spectra of trivalent RB_6's which we measured in this study are shown in Fig. 5(a). We can see that the absorption structure is observed around 0.6 eV for all RB_6's except LaB_6.

First, we attempt to estimate the intensity of this absorption. In general, the intensity of an optical absorption can be related to the effective electron number which contributes to the absorption. The absorption is seen to be apparently overlapping with the normal Drude structure. So we fitted the slope of the curve in the lower-energy region with the simple Drude model and estimated the intensity of the infrared absorption by subtracting the Drude curve from the measured curve. The fitted Drude curves are shown by dashed lines in Fig. 5(a). Figure 5(b) shows an example of the Drude fitting of GdB_6 in the low-energy part. Below 20 meV, the estimated error becomes larger than that in the high-energy region as shown in Fig. 5(b). So the fitting can be done exactly.

The estimated intensities of the infrared absorption (N_{IR}), the Drude absorption (N_D), and the sum of these absorptions (N_D+N_{IR}) are shown in Fig. 6. In this figure, each error bar shows the error of the reflectivity ($\pm1\%$) and the ambiguity in the Drude fitting. The integration range for N_D and N_{IR} was limited, only up to 2.1 eV. The error for the absolute value is estimated to be much less than 10% and the relative error among RB_6's is much less. LaB_6 was not able to be fitted by the simple Drude model as mentioned before. In the same sense, a similar deviation seems to occur in other RB_6's. This error for N_{IR} is evaluated to be 10% and 20% for the heavy and light RB_6 compounds, respectively. The same analysis was done for the all materials at 9 K. The results, however, are almost equal to those at 300 K within the experimental error. So we deal with the spectra only at 300 K. For example, in GdB_6 N_{IR} was 0.67 ± 0.10 f.u.$^{-1}$ at 300 K and 0.57 ± 0.07 f.u.$^{-1}$ at 9 K. GdB_6 is in the antiferromagnetic state at 9 K. The origin of the small difference of N_{IR} must be investigated further, to determine whether it originates from the magnetic transition or not.

In Fig. 6, we can see that N_{IR} increases almost in proportion to the $4f$ electron number from LaB_6 to GdB_6, but in contrast decreases above GdB_6. On the other hand, N_D decreases from LaB_6 to GdB_6, but increases above GdB_6 in the opposite way to N_{IR}. The sum of N_D and N_{IR} shows a slight decrease from LaB_6 to HoB_6.

Next, we consider the origin of the infrared absorption. It is certain that the occupied $4f$ electrons are closely related to this absorption because the fundamental elec-

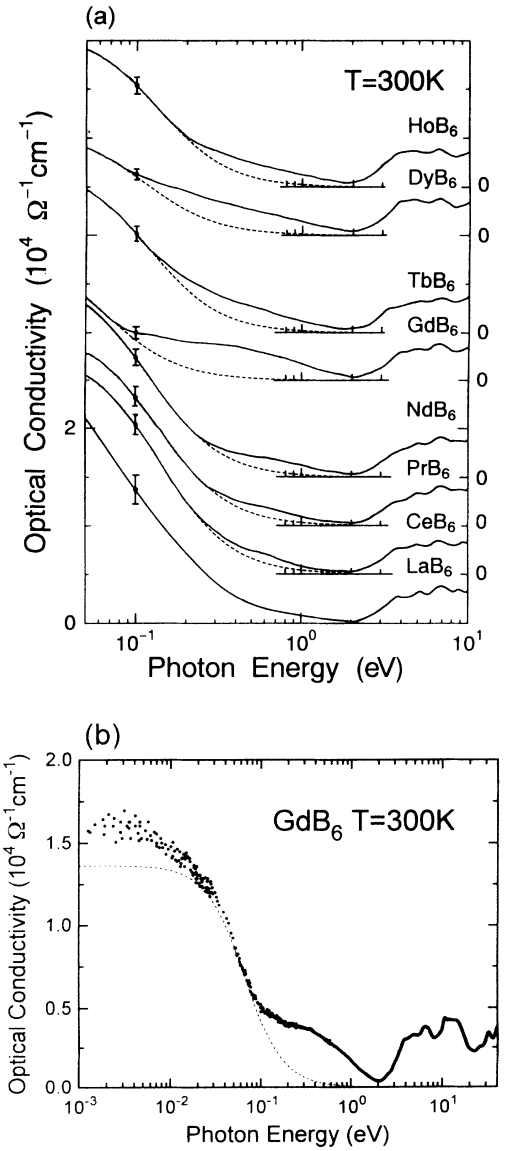

FIG. 5. (a) Optical conductivity spectra of RB_6(R=La, Ce, Pr, Nd, Gd, Tb, Dy, and Ho) at 300 K in the photon energy region from 50 meV to 10 eV (solid line). Dashed lines show the fitted Drude curves. (b) Optical conductivity spectrum (dotted line) of GdB_6 at 300 K in the photon energy region from 1 meV to 40 eV and fitted Drude function (dashed line).

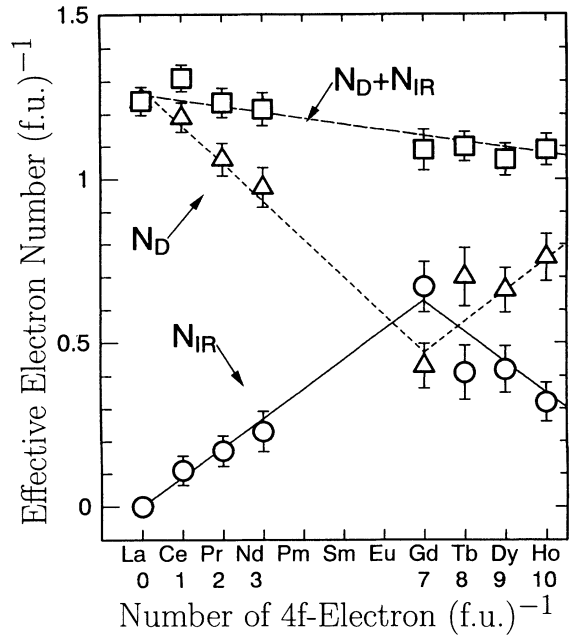

FIG. 6. Estimated effective electron number of the infrared absorption (N_{IR}), the Drude absorption (N_D), and the sum of these absorptions (N_D+N_{IR}). The error bars show the error of the intensity which originates from the error of the measured reflectivity and of Drude parameters.

tronic structure of RB_6 does not change but only the $4f$ bands change as the rare-earth element changes. It is also certain that the origin is due to absorption by conduction electrons because of the f-sum rule.

If the absorption is assumed to be due to interband transitions or the exciton of the $4f$-$5d$ transition, N_D alone becomes the number of conduction electrons. In this case, $m_D=2.4m_0$ in GdB_6, considering that $N_D=N\times(m_0/m_D)$, where N is the number of conduction electrons, m_0 the rest mass of the electron, and m_D the optical effective mass, and that all of these materials are monovalent metals. This value is three times larger than $0.8m_0$ of LaB_6 and this is contrary to the fact that the conduction band of each material has almost the same structure. Therefore we may consider that another term in addition to N_D may contribute to the number of conduction electrons. Note that the m_D of LaB_6 is almost equal to the effective mass of $0.6m_0$–$0.7m_0$ which is estimated by band calculation[24] and de Haas–van Alphen measurement.[25]

Let us consider the case that the sum of N_D+N_{IR} corresponds to the number of conduction electrons. N_D+N_{IR} is almost constant among all the materials as seen in Fig. 6. This results from the constant energy position of the plasma edge. These materials have the same number of conduction electrons, as mentioned before. So we may say that N_{IR} is a part of the number of conduction electrons and the absorption at 0.6 eV is due to conduction electrons. Before, we mentioned that the infrared absorption originates from the $4f$ electrons. Therefore the infrared absorption is thought to be due to the relation between conduction and $4f$ electrons, i.e, it is thought to originate from the interaction between the $4f$ and the conduction electrons.

In Fig. 6, we can clearly see that N_D+N_{IR} gradually decreases as the $4f$ electron number increases. This means that the optical mass (m_D) increases as the number of $4f$ electrons increases because all of these materials are monovalent metals. This is considered to be because the conduction band approaches the valence band as the atomic number increases. We can explain the origin of the increase of m_D from LaB_6 to YB_6, which is a reference material for the heavy RB_6 compounds, as follows. In YB_6, $m_D=1.01m_0$ because $N_D=0.99$ f.u.$^{-1}$. This value is larger than that of LaB_6. This is because the overlapping between the conduction band and the valence band of YB_6 is larger than that of LaB_6, as shown by the calculated band structures of LaB_6 (Ref. 24) and YB_6.[26] Note that the effective mass of the conduction electron originates from the energy position of the $4f$ band in general. In LaB_6, however, the unoccupied $4f$ state is known to be located at the far energy position of about 6 eV about the Fermi level.[8] So the contribution of the $4f$ band to m_D is small. It is considered that the boron $2s,2p$ bonding state mainly contributes to m_D. Therefore the m_D of YB_6 may become larger than that of LaB_6 because the conduction and the valence bands of YB_6 are hybridized more strongly than in LaB_6. The lattice constant of YB_6 is almost the same as that of the heavy RB_6 compounds from GdB_6 to HoB_6. So the conduction band of heavy RB_6 compounds is thought to go down in energy as in YB_6. Therefore m_D becomes larger with the heavier RB_6 compounds.

From the discussion of the origin of N_{IR}, it is important to define what the conduction-electron absorption is and what the interband absorption is. As mentioned in our previous paper, the interband transition which begins from 2 eV was assigned to be the transition from the top of the B $2s,2p$ bonding band with a large density of states to the unoccupied conduction band.[8] The first peak of absorption at 3.7 eV was identified as the transition from the first peak in the density of states of the B $2s,2p$, bonding state at 3 eV below the Fermi energy to the first peak of the unoccupied conduction band at 1.5 eV above the Fermi energy.[8] It was argued that this energy difference is decreased and the intensity is enhanced by the virtual-exciton effect. Note that such a virtual-exciton effect has been emphasized to be essentially important to understand the gap state in SmB_6.[27] The transition from the $4f$ to the $5d$ states and the opposite one appear at a higher energy than 2 eV except for SmB_6.[8] On the other hand, conduction-electron absorption means the process in which the initial state is the occupied conduction band. Then, by the f-sum rule, the intensity should be nearly the same for all the trivalent RB_6 compounds under consideration. This consideration identifies the infrared absorption as due to the conduction band. The narrow localized character of the infrared absorption suggests that this process is also a virtual-exciton-like process. Then the only possibility is the transition from the saddle point of Σ_1 to the saddle points of Γ_{12} and Γ_{25} existing at the

first peak of the density of states.[24] Because of the saddle points, this transition is expected to be a virtual-exciton-like one which lowers the excitation energy from 1.5 to 0.6 eV and enhances the intensity. The expected electronic transition from which the infrared absorption originates is shown in Fig. 7. This process cannot be a direct transition because there are no corresponding band states above the necks.

Because the $5d$-$4f$ intra-atomic Coulomb exchange interaction is much stronger than the electron-phonon interaction, the former should be the main origin of this indirect transition. For GdB_6, the usual spherical exchange interaction $I_{df}\mathbf{S}_f\cdot\mathbf{S}_d$ is the dominant interaction. Here $\mathbf{S}_d$ and $\mathbf{S}_f$ denote the $5d$ and $4f$ spin angular momenta, respectively. Because the transition is proportional to the square of this interaction, this cannot explain the observed $\langle \mathbf{S}_f \rangle$ linear dependence. For the light rare-earth compounds, the quadrupole interaction is the main key to solving the discrepancy. In CeB_6, it was calculated that the inverse lifetime due to quadrupole scattering is several times larger than that of the spherical exchange interaction.[26] In PrB_6, they are nearly equal and even in NdB_6 the quadrupole scattering has a substantial contribution. Our experimental result is actually explained satisfactorily. For the heavy RB_6 compounds, the inverse lifetime of TbB_6 is consistent with the square dependence of $\langle \mathbf{S}_f \rangle$ but the results for DyB_6 and HoB_6 are anomalous. This is again explained by an anomalous quadrupolar interaction. It is well known that crystals of the heavy RB_6 compounds are unstable because the atomic size of the heavy rare earth is too small. Indeed it was observed in DyB_6 and HoB_6 that the $4f$ quadrupolar interaction couples strongly with the lattice quadrupolar interaction, causing various anomalies.[28] The anomalous enhancement HoB_6 and DyB_6 is thought to be related with this mechanism. For a more detailed quantitative evaluation, however, more extensive studies are needed.

The infrared absorption is seen not only in RB_6 but also in Gd monochalcogenides as shown by Beckenbaugh *et al.*[29] From the reflectivity spectra of GdS, GdSe, and GdTe, the infrared absorption of these materials has almost the same magnitude as that of GdB_6. The rare-earth monochalcogenide RX has a similar band structure to RB_6. RX for a trivalent R is also a monovalent metal and has the conduction-band bottom at each X point in the Brillouin zone. Therefore there are also saddle points at the Γ point above the Fermi energy and at the neck below the Fermi energy. In fact, Vlasov and Farberovich calculated the LaS band structure[30] and found a similar neck structure between the Γ and W points. Takegahara also derived a similar band structure of RX (R = La,Gd and X = S,Se,Te).[31] Therefore the corresponding infrared absorption may occur for the same reason in RB_6.

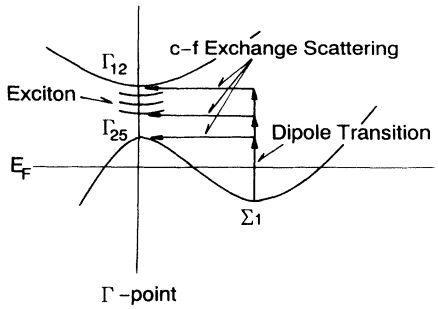

FIG. 7. Possible mechanism to explain the origin of the infrared absorption in the band structure of LaB_6.

C. Absorption structure of SmB_6

In SmB_6, the absorption structure which is seen in trivalent RB_6 compounds below 2 eV is also observed (Fig. 8), but the intensity seems to be larger than in trivalent RB_6's. At 300 K, Drude-type conduction-electron absorption is observed, but another absorption peak is seen around 0.5 eV. Below 20 K, this material has an energy gap of about 14 meV. So there are few conduction electrons in this material below 20 K. At 13 K, two peaks appear in place of one broad peak at 300 K. From the comparison between these shapes and intensities, the spectrum at 13 K seems to have lower thermal broadening than at 300 K, so we discuss the intensity of the absorption at 13 K.

At 13 K, we can estimate that the effective electron number below 2 eV is 0.79 f.u.$^{-1}$ using the integral of the optical conductivity as mentioned before. It is certain that the absorptions due to the transition from the $4f$ to the $5d$ states and the opposite case are included in the estimated value. The reason is that the occupied $4f$ states in Sm^{2+} ion and the unoccupied $4f$ states in Sm^{3+} ion are located near the Fermi level, as observed in the photoemission of SmB_6 (Ref. 32) and the inverse photoemission of Sm metal.[33]

We consider the transition from $4f$ to $5d$ states. The $4f$ states after photoemission are the three symmetric states ^6F, ^6H, and ^6P. But only ^6F and ^6H states are able to contribute to the absorption below 2 eV. In fact, the splitting energy between double peaks in the optical conductivity spectrum is consistent with the splitting energy

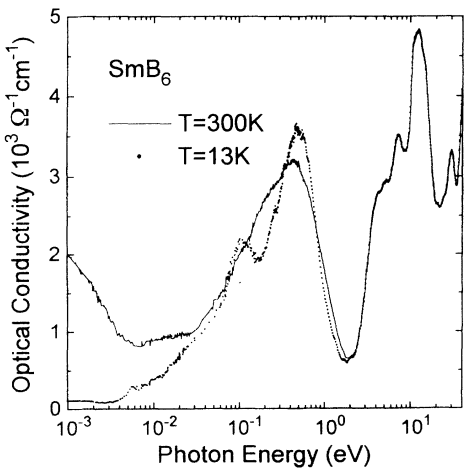

FIG. 8. Optical conductivity spectra of SmB_6 at 300 (solid line) and 13 K (dotted line).

between ^6F and ^6H states in the photoemission data.[32] The electron number in the ^6F and ^6H states is estimated to be about 1.8 f.u.$^{-1}$. The $5d$ density of states near the Fermi level is almost constant at 0.10 states f.u.$^{-1}$eV^{-1}spin^{-1} from the band structure. So the $5d$ state number becomes 0.20 f.u.$^{-1}$spin^{-1}. Therefore the effective electron number of the transition from $4f$ to $5d$ states is estimated at 0.20 f.u.$^{-1}$, because the oscillator strength of the $4f$-$5d$ transition is about 0.55,[7] the integral upper limit of the energy is 2 eV, and the conservation of spin must be included in the optical absorption.

The $5d$-$4f$ transition is considered in the same way. The number of $4f$ unoccupied states is estimated as 1.3 f.u.$^{-1}$spin^{-1}. The state number of the $5d$ initial state is about 0.20 f.u.$^{-1}$spin^{-1}. Therefore the estimated intensity of the absorption from $5d$ to $4f$ states is concluded to be 0.14 f.u.$^{-1}$. In this case, the oscillator strength of the $5d$-$4f$ transition is assumed to be the same as for the $4f$-$5d$ transition.

Consequently the sum of the intensities of the $4f$-$5d$ transition and the opposite one becomes 0.34 f.u.$^{-1}$ So we can get the intensity of 0.45 f.u.$^{-1}$ which is the difference between 0.79 f.u.$^{-1}$ for the total absorption below 2 eV and 0.34 f.u.$^{-1}$ for sum of the intensities of the $4f$-$5d$ and $5d$-$4f$ transitions. This value is in perfect agreement with the line of N_{IR} in Fig. 6.

This result is thought to mean that the same infrared absorption of trivalent RB_6's exists in SmB_6. Therefore it is thought that the infrared absorption due to the transition between neck points of Σ_1 and Γ_{12} is not seen only in trivalent RB_6 but also in SmB_6. It is thought that the Fermi level of SmB_6 is located at the same energy position as in trivalent RB_6's and SmB_6 has a similar band structure to trivalent RB_6. But further investigation of the Fermi level of SmB_6 must be done.

V. CONCLUSIONS

In this paper, we report the absorption structure due to the conduction electrons of trivalent RB_6's (R =La, Ce, Pr, Nd, Gd, Tb, Dy, Ho, and Y) and mixed-valent SmB_6. The following results were critically discussed and explained. (1) The measured optical conductivity spectra in LaB_6 and YB_6, which are typical monovalent metals with no occupied $4f$ electron states, were unable to be fitted by the simple Drude model. This is mainly attributed to a frequency-dependent relaxation time. In the low-frequency region, this was attributed to the electron-phonon scattering and in a higher-frequency region to electron-electron scattering. (2) It was found that the effective electron number below the plasma edge of about 2 eV in trivalent RB_6's decreases gradually as the atomic number increases. This reason is thought to be that the effective mass of the conduction electrons becomes heavier in the heavy RB_6 compounds because the overlapping between the conduction and the valence bands increases as R becomes heavy. (3) We found an absorption structure around 0.6 eV, which is common to all the materials and of which the intensity is nearly proportional to the $4f$ spin angular momentum. From the band structure of LaB_6, interband transitions or the virtual exciton from the saddle points of Σ_1 to the neck point of Γ_{12} and Γ_{25}, assisted by the scattering of the intra-atomic $5d$-$4f$ Coulomb exchange interaction, seem to be the most probable origin of the infrared absorption. To explain the observed $\langle S_f \rangle$ dependence of N_{IR}, the $4f$ quadrupole scattering for light R and the lattice quadrupolar scattering for the heavy R due to crystal instability should be considered. (4) In SmB_6, the similar absorption structure below 2 eV to that in trivalent RB_6 was also observed. The absorption structure was seen to consist of two parts, one due to the transition from $4f$ to $5d$ states and the opposite one and the other due to the same absorption which is seen in trivalent RB_6's. The latter absorption intensity perfectly fits with the line of N_{IR}. This can be interpreted that the Fermi level is located at the same position as in trivalent RB_6.

ACKNOWLEDGMENTS

The authors would like to thank the staffs of the UVSOR facility in the Institute of Molecular Science and of the SOR-RING in the Institute for Solid State Physics, the University of Tokyo, for their assistance through this research. One of them (S. Kimura) acknowledges Professor M. Ikezawa of Tohoku University for his encouragement. This research was supported in part by a Grant-in-Aid for Scientific Research on Priority Areas by the Ministry of Education, Science and Culture of Japan.

[1]T. Komatsubara, N. Sato, S. Kunii, I. Oguro, Y. Furukawa, Y. Onuki, and T. Kasuya, J. Magn. Magn. Mater. **31-34**, 368 (1983).

[2]T. Kasuya, M. Kasaya, K. Takegahara, T. Fujita, T. Goto, A. Tamaki, M. Takigawa, and H. Yasuoka, J. Magn. Magn. Mater. **31-34**, 447 (1983).

[3]Z. Fisk, D. C. Johnston, B. Cornut, S. von Molnar, S. Oseroff, and R. Calvo, J. Appl. Phys. **50**, 1911 (1979).

[4]E. Kierzek-Pecold, Phys. Status Solidi **33**, 523 (1969).

[5]V. N. Gurin, M. M. Korsukova, M. G. Karin, K. K. Sidorin, I. A. Smirnov, and A. I. Shelykh, Fiz. Tverd. Tela (Leningrad) **22**, 715 (1980) [Sov. Phys. Solid State **22**, 418 (1980)].

[6]G. Travaglini and P. Wachter, Phys. Rev. B **30**, 5877 (1984).

[7]S. Kimura, T. Nanba, S. Kunii, and T. Kasuya, J. Phys. Soc. Jpn. **59**, 3388 (1990).

[8]S. Kimura, T. Nanba, M. Tomikawa, S. Kunii, and T. Kasuya, Phys. Rev. B **46**, 12 196 (1992).

[9]S. Kimura, T. Nanba, S. Kunii, and T. Kasuya, J. Phys. Soc. Jpn. **61**, 371 (1992).

[10]S. Kimura, T. Nanba, S. Kunii, T. Suzuki, and T. Kasuya, Solid State Commun. **75**, 717 (1990).

[11]K. Segawa, A. Tomita, K. Iwashita, M. Kasaya, T. Suzuki, and S. Kunii, J. Magn. Magn. Mater. **104-107**, 1233 (1992).

[12]H. C. Longuet-Higgins and M. de Roberts, Proc. R. Soc. Lon-

don **224**, 336 (1954).
[13]K. Iwashita, T. Matsumura, K. Segawa, and S. Kunii, Physica B **186-188**, 636 (1993).
[14]T. Nanba, Rev. Sci. Instrum. **60**, 1680 (1989).
[15]F. Wooten, *Optical Properties of Solids* (Academic, New York, 1972).
[16]M. Cardona and D. L. Greenaway, Phys. Rev. **133**, A1685 (1964); M. Cardona, *ibid.* **140**, A651 (1965).
[17]J. B. Smith and H. Ehrenreich, Phys. Rev. **138**, B923 (1982).
[18]R. T. Beach and R. W. Christy, Phys. Rev. B **16**, 5277 (1977); G. R. Parkins, W. E. Lawrence, and P. W. Christy, *ibid.* **23**, 6408 (1981).
[19]W. H. Weber and S. L. McCarthy, Phys. Rev. B **12**, 5643 (1975); A. J. Sievers, *ibid.* **22**, 1600 (1980); H. Gugger, M. Jurich, and J. D. Swalen, *ibid.* **30**, 4189 (1984).
[20]L. D. Landau, Zh. Eksp. Teor. Fiz. **30**, 1058 (1956) [Sov. Phys. JETP **3**, 920 (1957)]; **32**, 59 (1957) [**5**, 101 (1957)].
[21]C. Julien, J. Ruvalds, A. Virosztek, and O. Gorochov, Solid State Commun. **79**, 875 (1991).
[22]K. Takegahara and T. Kasuya, Solid State Commun. **53**, 21 (1985).
[23]T. Tanaka, T. Akahane, E. Bannai, S. Kawai, N. Tsuda, and Y. Ishizawa, J. Phys. C **9**, 1235 (1976).
[24]A. Hasegara and A. Yanase, J. Phys. F **7**, 1245 (1977); H. Harima, O. Sakai, T. Kasuya, and A. Yanase, Solid State Commun. **66**, 603 (1988).
[25]Y. Ishizawa, T. Tanaka, E. Bannai, and S. Kawai, J. Phys. Soc. Jpn. **42**, 112 (1977); Y. Onuki, T. Komatsubara, P. Reinders, and M. Springford, *ibid.* **58**, 3698 (1989).
[26]Y. Aoki, Ph.D. thesis, Tohoku University, 1982 (in Japanese).
[27]T. Kasuya, J. Phys. Soc. Jpn. **63**, 397 (1994).
[28]S. Kunii (unpublished).
[29]W. Beckenbaugh, J. Evers, G. Gütherodt, E. Kaldis, and P. Wachter, J. Phys. Chem. Solids **36**, 239 (1975).
[30]S. V. Vlasov and O. V. Farberovich, Solid State Commun. **56**, 967 (1985).
[31]K. Takegahara (unpublished).
[32]J.-N. Chazalviel, M. Campagna, G. K. Wertheim, P. H. Schmidt, and Y. Yafet, Phys. Rev. Lett. **37**, 919 (1976); M. Champagna, G. K. Wertheim, and Y. Bear, in *Photoemission in Solids II*, edited by L. Ley and M. Campagna (Springer-Verlag, Berlin, 1979), p. 245.
[33]J. K. Lang, Y. Bear, and P. A. Cox, J. Phys. F **11**, 121 (1981).